Int. Journ. of Wettability Science and Technology, Vol. 1, pp. 221–230
Reprints available directly from the publisher.
Photocopying permitted by license only.

Behaviour of laser treated with water droplet on carbon nanotubes coated silicon surface

C. WANG, G. ZHANG, L. WANG, Q.G. WANG, X.C. LU AND W. YAO*

Department of Space Sciences, Qian Xuesen Laboratory of Space Technology, China Academy of Space Technology, Beijing 100094, China.

Laser processing is a promising method for the modification and micro/nano structuring of solid surfaces. The key factors which greatly affect the quality of laser processing are the size of heat-affected zones (HAZ) and surface debris. A water droplet assisted laser processing method on carbon nanotube (CNT) coated surfaces is proposed in this paper. The static contact angle (CA) and fragmentation induced by laser of the water droplet on the surface of the system are conducted by experiment. The results reveal that the surface of silicon can be changed from hydrophilic to hydrophobic by introducing CNT coatings and the CA of water droplet increases with the coating layers of CNTs. The water droplets, which behaved as a focusing lens, could obviously enhance the laser intensity underneath the water droplet. It was found that the smaller water droplets show a much better focusing effect. The experimental results show the proposed method has great potential to reduce the size of HAZ and removes the spatter generation.

Keywords: Laser processing, carbon nanotubes, water droplet, contact angle, fragmentation

1 INTRODUCTION

Laser processing is a promising method for the modification and micro/nano structuring of solid surfaces [1-6]. Among different types of lasers, short pulsed lasers have a wide current application base and potential for further industrial applications [7]. The interaction between lasers and mate-

*Corresponding author: e-mail: yaowei@qxslab.cn

rials is very complicated due to the ultra-transient heat transfer process and several influence factors, such as machining medium, laser parameters and material parameters. The mechanism of laser-material interaction mainly depends on the thermal effects, especially the heat-affected zone (HAZ) and the molten phase [8, 9]. The formation of HAZ can generate heat damage in solid materials by induced thermal stress [10]. Furthermore, the deposit, recasting and spattering irregularly of the molten phase may reduce the processing quality and precision [11]. Material ablation with minimum debris and HAZ with low processing cost is one of the main challenges for the successful implementation of laser micromachining as a competitive technology in this field [12]. Accordingly, considerable studies have been carried out, and several strategies such as ultra-short pulsed lasers [13, 14], inert gas assisted laser processing [15, 16], ultrasonic-aided laser drilling [17] and chemical assisted laser machining [18] have been developed to resolve the problems.

Ultra-short pulsed (picosecond or femtosecond) lasers, as promising alternatives for machining ceramics, can effectively minimize the size of HAZs, as the thermal diffusion is highly restricted within the extreme short laser material interaction time [19]. Kurita *et al.* [20] found that femtosecond lasers could reduce the HAZs compared to nanosecond laser. However, ceramics engineered with femtosecond lasers can only be used in the mainstream once femtosecond laser systems reduce in cost and when there are improvements made to with regards to processing efficiency problems. Some studies demonstrated that the formed debris resulting from the femtosecond laser ceramic machining is hard to remove [21]. Water assisted laser machining, as an advanced manufacturing method, can avoid or reduce the HAZs and debris re-deposition [22]. The effect of the water during laser material processing can convert the light energy into a mechanical impulse, producing higher plasma pressure and longer duration of shock waves due to confinement [23]. However, they also observed that the shielding effect was induced by filamentation and optical breakdown of water, which reduced the amount of energy reaching the target [24]. Furthermore, the laser beam could be scattered by laser induced gas bubble, affecting the precision of the processed surface [25].

In this paper, pulse laser processing assisted by water droplets is further investigated on a carbon nanotube (CNT) coated silicon system. Static contact angles and pulse laser induced fragmentations of water droplets on the CNT coated silicon surface were carefully measured. The relationships between the volume of water droplets and the duration of laser irradiation, giving rise to the shattering time of water droplets were analyzed. Specifically, the shattering time of water droplets will be much shorter with the decrease of the volume of water droplets when the laser output power remains constant. This indicates that the effect of a focusing lens consisting of smaller water droplets will give rise to an enhanced sharpness in focus. It is believed

that our results will provide important reference to the improvement of water droplet-assisted laser machining.

2 EXPERIMENTAL TECHNIQUE

The experimental systems are divided into two parts: the static contact angle test system and the water droplets fragmentation test system.

2.1 Static contact angle measurement of CNTs coated silicon surfaces

As illustrated in Figure 1, the experimental set-up for the static contact angle measurements mainly used a contact angle meter (POWEREACH, JC2000D4M), a micro-injector (Microliter Syringes, 5 μl), test samples and a data collector. The surface of the silicon wafer was polished and the silicon wafers has a thickness of 600 μm. The super-aligned CNT films were pulled out from the super-aligned CNT arrays, which were synthesized on silicon substrates by low-pressure CVD. Acetylene or ethylene was used as the precursor, and the resulting silicon wafers were used as the substrates. The growth temperatures and the growth time were in the range of 650−700 °C and 5−20 min, respectively. The height of the super-aligned CNT arrays could be altered from 100 to 900 μm, dependant on the growth time. The diameters of the CNTs ranged between 10-20 nm and most of the CNTs were multi-walled. Different layers (1, 3, 5, 7-layer) of CNTs were spread on the silicon wafer, and the thickness of the monolayer CNTs was of the order of tens of nanometers. The volume of a water droplet, which was

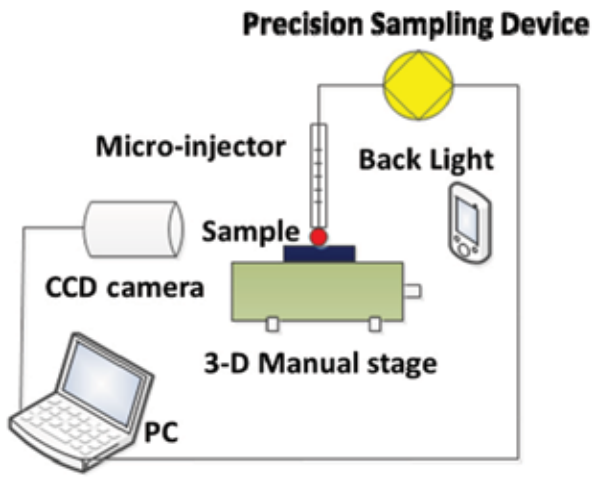

FIGURE 1
Schematic diagram of the contact angle test system.

about 1 µl, was controlled by a micro injector and a stepping motor. The contact angle of water droplets on the CNT coated silicon was measured by the contact angle meter and the associated software. The water used was deionized water (conductivity ~0.1 µS/cm) and all tests were done at room temperature (about 20°C).

2.2 Fragmentation of water droplet induced by the pulse laser

As shown in Figure 2, the experimental set-up for the fragmentation of water droplets induced by the pulse laser was comprised of a short pulsed laser, a digital delay generator, a high speed CCD camera, several lenses, an LED backlight, a three-dimensional stage and the tested samples. The wavelength, the minimum pulse duration, the output power and the radius of focusing spot of the pulsed laser (BWT BEIJING LTD, DS3-11312-103-K793DW13RN-30W) were 792 nm, 20 µs, 30 W and 100 µm, respectively. The temporal distribution of the laser pulses could be switched between continuous and pulse modes. The switch instructions of the laser and the CCD camera were controlled by a digital delay generator (RIGOL, DG1022U). The fragmentation shape of the water droplets was recorded by a high-speed CCD camera (Phantom v1611). A resolution of 1280 x 800 was used with a recording speed of 3000 frames per second in the present experiment. An LED light source was used as the supplementary lighting in the high speed imaging. The brightness of the light source was regulated by a DC low-voltage power sup-

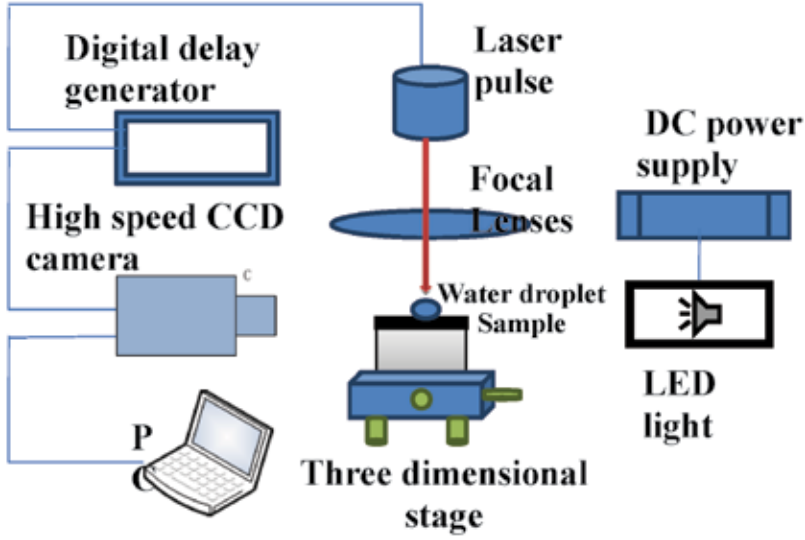

FIGURE 2
Schematic diagram of the experimental system for fragmentation of water droplet induced by the pulse laser.

ply (Keysight, N5750A). A three dimensional stage (Daheng Optics) was used to adjust the focusing location and distance from laser spot and water droplet.

The sample used in this experiment was the 5-layer CNT coated silicon. The water was deionized water (conductivity ~0.1 μS/cm) and the volumes of the water droplets were approxiamtely 0.5 μl, 1.0 μl and 1.5 μl, controlled by a micro-injector (Microliter Syringes, 5 μl). The experiments were conducted in open conditions at room temperature (about 20°C), in a standard atmosphere with approximately 60% relative humidity.

3 RESULTS AND DISCUSSIONS

3.1 Contact angles of droplets on different samples

Figure 3(a) shows a photograph of the pure silicon wafer and the 3-layer CNT coated silicon wafer. It can be seen that the silicon surface colour changed with the addition of the CNTS and the CNTs were coated very well onto the polished silicon material. SEM images of the silicon surface with CNT coating can be seen in previous work [26]. Furthermore, the morphologies of the CNT coated silicon surfaces were characterized by optical microscopy, which is shown in the Figure 3(b). The CNT coatings contained a lot of interspaces and the silicon was partly covered. These CNTs have relatively low surface energy and formed periodic micro-scale columns, resulting in the hydrophobic properties of the CNT surface.

The static contact angles of the polished surfaces of pure silicon are shown in Figure 4(a-e). The experimental results revealed that the surface of the silicon could be changed from exhibiting a hydrophilic property to a hydrophobic property because of the coatings of CNTs. Specifically, the contact angles of water droplets on different samples increased with the thickness of CNTs. For example, the contact angle of a water droplet on the pure silicon

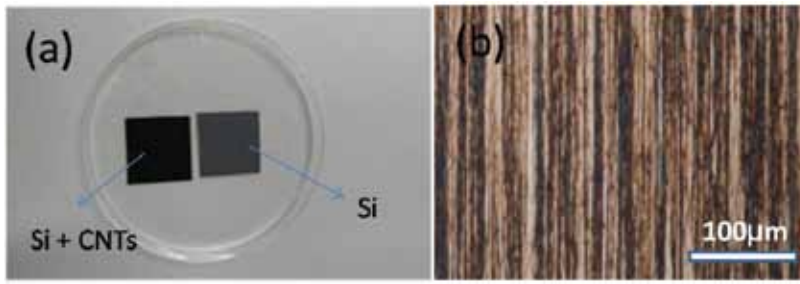

FIGURE 3
(a) Photographs of pure silicon surface and the 3-layer CNT coated silicon surface; (b) Microscope photos of the silicon surface coated by the 3-layer CNTs.

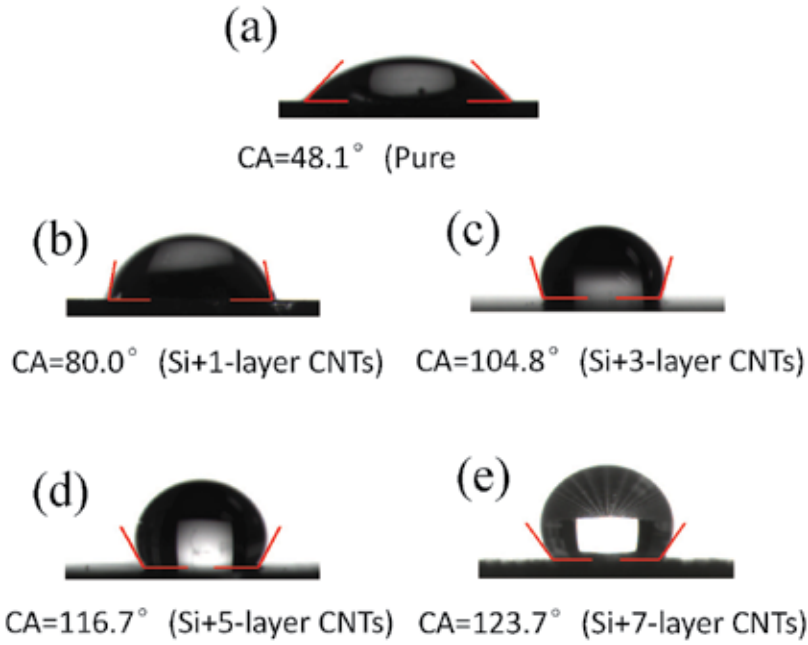

FIGURE 4
Contact angles of water droplets on (a) the pure silicon surface and (b-e) the different thickness of CNT coated silicon surfaces.

surface was 48.1°, which indicated a hydrophilic property of the pure silicon surface. The contact angles of water droplets on the silicon surfaces with 1, 3, 5, 7 CNT layers was 80.0°, 104.8°, 116.7° and 123.7°, respectively. This shows the transition from the hydrophilic property to a hydrophobic property.

3.2 Ablation of CNTs and fragmentation of water droplets induced by a pulse laser

The morphologies of incipient combustion of the 5-layer CNT coated on silicon surface and the fragmentation of water droplets with different volumes (0.5 µl, 1.0 µl and1.5 µl) induced by continuous laser with output power 30 W are shown in Figure 5(a-c), Figure 5(d-f) and Figure 5(g-i), respectively.

When the water droplets on the 5-layer CNT coated silicon surface were irradiated by the pulsed laser with a constant output power, the temperature of the CNTs would continually rise until point was reached for an incipient combustion state. The combustion of CNTs could obviously change the interfacial tensions between water droplets and CNT coated surface, and then induce the fragmentation instability of water droplets. However, the cooling effect of water droplets would limit the burning level of CNTs, and the absorbing heat from CNTs could not satisfy the

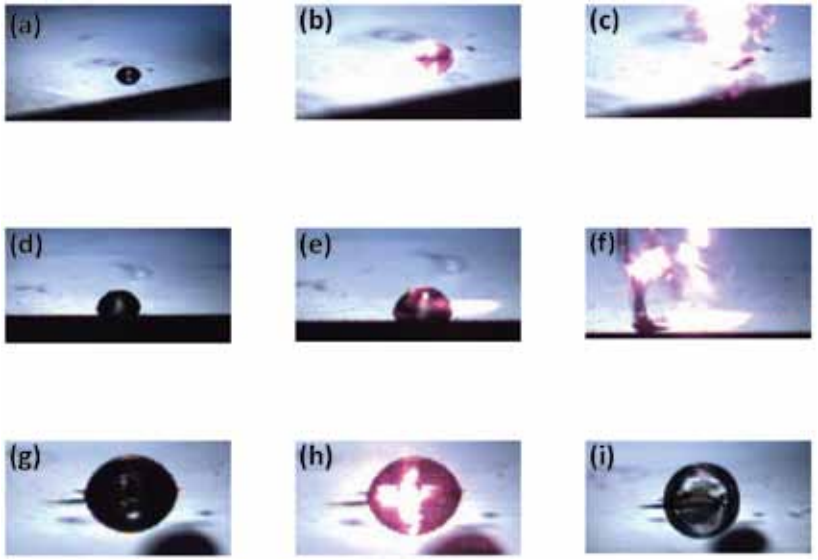

FIGURE 5
(a- c) Morphologies of ablation of CNTs and fragmentation of the 0.5 μl water droplets; (d-f) Morphologies of ablation of CNTs and fragmentation of the 1.0 μl water droplets; (g-i) Morphologies of ablation of CNTs and fragmentation of the 1.5 μl water droplets.

condition of fragmentation instability for larger volumes of water droplets. So there is a critical fragmentation volume of water droplets to a constant thickness of CNT coating.

In the initial stages of the CNTs burning and fragmentation of water droplets were record by CCD camera and are shown in Figure 6. These results demonstrated that, when water droplets, located on the CNT coated silicon surface, are irradiated by the pulsed laser, the combustion of CNTs firstly occurs, and the fragmentation instability of water droplets subsequently takes place. For the same thickness CNT coated sample, the time of incipient combustion of CNTs with a smaller water droplet is much faster. So the effect of a focusing from the water droplets enhanced the sharpness of the focus. The fragmentation instability of droplets could not be induced by a time increase in laser irradiation when the volume of water droplet exceeded one critical value.

The HAZ and surface debris induced by laser irradiation of the water droplets on the surface of CNT coated silicon are shown in Figure 7. It was found that the HAZ was the shape of a circle and the radius was small and distribution was uniform. The diameter of spot focused by the water droplet, as shown in the centre part of Figure 7(a), was about one half of the laser irradiation point and so the focusing effect of water droplet was very clear.

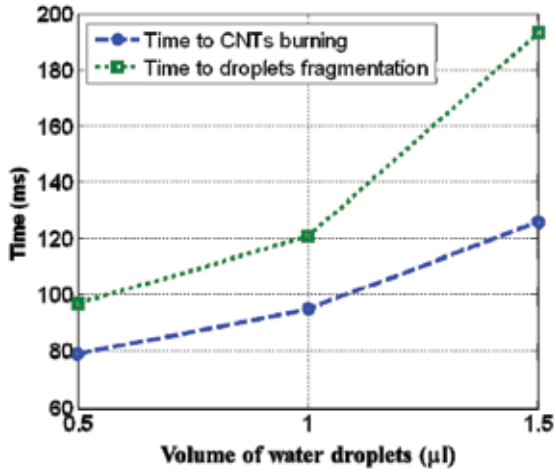

FIGURE 6
Initial time of CNTs incipient combustion and water droplet fragmentation.

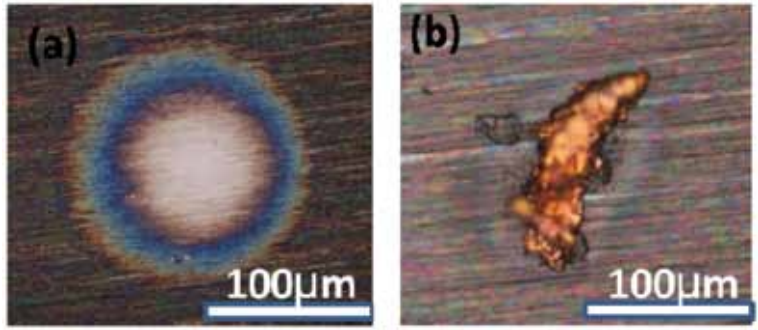

FIGURE 7
Morphologies of (a) HAZ and (b) surface debris.

The distance of the HAZ from the machined hole was narrow and the distribution was uniform because of the instant cooling down effect of the water droplet. This possibly showed that the laser absorption ratio and ability of silicon were all enhanced by the water droplet. The surface debris, as shown in Figure 7(b), mainly was the combustion product of the CNTs, and had a long distance (around hundreds of micrometers) from the machining spot. This surface debris could also be cleaned easily. The water droplet fragmentation was the main driver to removing the surface debris from the machining spot location.

4 CONCLUSIONS

In the present work, a water droplet assisted laser processing method on CNT coated silicon surfaces is proposed. The static contact angle (CA) and fragmentation induced by laser of water droplet on the surface of the system are conducted by experiment. Based on the results and discussion, the following conclusions can be drawn:

1. The CNT coatings could change the surface characteristics of silicon from hydrophilic to hydrophobic with the CNT layers. The contact angle of water droplet on the silicon surface increased with the increase in CNT layers.
2. Water droplets on CNT coated surfaces act as a focusing lens to enhance the absorbing laser intensity and minimize the HAZ. The size of the water droplet plays an important role to improve the focusing effects and fragmentation instability of the water droplet.
3. There is a critical fragmentation volume of water droplets to a constant thickness of CNT coating.
4. The proposed water droplet assisted laser processing method on CNT coated surfaces can effectively reduce the HAZ and be used to enhance the cleanability of surface debris.

REFERENCES

[1] Trtica M. and Gakobic B., Pulsed TEA CO_2 laser surface modification of silicon. *Applied Surface Science* **205** (2003), 336-342.

[2] Hong L., Rusli, Wang L., Zheng H.Y., Wang H. and Yu H.Y., Femtosecond laser fabrication of large-area periodic surface ripple structure on Si substrate, *Applied Surface Science* **297** (2014), 134-138.

[3] Li B., Zhou M., Zhang W., Amoako G. and Gao C-Yu., Comparison of structures and hydrophobicity of femtosecond and nanosecond laser-etched surfaces on silicon. *Applied Surface Science* **263** (2012), 45-49.

[4] Subramonian S., Kasim M., Ali M., Abdullah R.I.R. and Anand T.J.S., Micro-drilling of silicon wafer by industrial CO2 laser. *International Journal of Mechanical and Materials Engineering* **10** (2015), 2.

[5] Yao C., Alvarado J., Marsh C., Jone B.G. and Collins M.K., Wetting behavior on hybrid surfaces with hydrophobic and hydrophilic properties. *Applied Surface Science* **290** (2014), 59-65.

[6] Hou Y., Yu M., Chen X., Wang Z. and Yao S., Recurrent filmwise and dropwise condensation on a beetle mimetic surface. *ACS Nano* **9** (2014), 71-81.

[7] Fu Z., Wu B., Gao Y., Zhou Y. and Yu G., Experimental study of infrared nanosecond laser ablation of silicon: The multi-pulse enhancement effect. *Applied Surface Science* **256** (2010), 2092-2096.

[8] Lu Q., Mao S., Mao X. and Russo E., Theory analysis of wavelength dependence of laser-induced phase explosion of silicon. *Journal of Applied Physics* **104** (2008), 083301-7.

[9] Charee W., Tangwarodomnukun V. and Dumkum C. Laser ablation of silicon in water under different flow rates. *The International Journal of Advanced Manufacturing Technology* **78** (2015), 19-29.

[10] Heinrich G., Bähr M., Stolberg K., Wutherich T., Leonhardt M. and Lawrenz A., Investigation of ablation mechanisms for selective laser ablation of silicon nitride layers. *Energy Procedia* **8** (2011), 592–597.

[11] Yoshida T., Yamada Y., Suzuki N., Makino T., Orii T. and Onai S., Semiconductor nanocrystallite formation using inert gas ambient pulsed laser ablation and its application to light emitting devices. *Proceedings of SPIE* **3618** (1999), 71-81.

[12] Lauzurica S. and Molpeceres C., Assessment of laser direct-scribing of a-Si:H solar cells with UV nanosecond and picosecond sources. *Physics Procedia* **5** (2010), 277-284.

[13] Chichkov B., Momma C., Nolte S., Alvensleben F. von. and Tunnermann A., Femtosecond, picosecond and nanosecond laser ablation of solids. *Applied Physics A: Materials Science & Processing* **63** (1997), 109-115.

[14] Rogers M., Grigoropoulos C., Minor A., and Mao S.S., Absence of amorphous phase in high power femtosecond laser-ablated silicon. *Applied Physics Letters* **94** (2009), 011111.

[15] Rao B., Kaul R., Tiwari P. and Nath A.K., Inert gas cutting of titanium sheet with pulsed mode CO2 laser. *Optics and Lasers in Engineering* **43** (2005), 1330-1348.

[16] Hong L., Zhang Y. and Mi C., Technological study of laser cutting silicon steel controlled by rotating gas flow. *Optics and Laser Technology* **41** (2009), 328-333.

[17] Lau W., Yue T. and Wang M., Ultrasonic-aided laser drilling of aluminum-based metal matrix composites. *CIRP Annals* **43** (1994), 177-180.

[18] Li L. and Achara C., Chemical assisted laser machining for the minimisation of recast and heat affected zone. *CIRP Annals* **53** (2004), 175-178.

[19] Amera M.S., El-Ashry M.A., Dosser L.R., Hix K.E., Maguire J.F. and Irwin B., Femtosecond versus nanosecond laser machining: comparison of induced stresses and structural changes in silicon wafers. *Applied Surface Science* **242** (2005), 162–167.

[20] Kurita T., Komatsuzaki K. and Hattori M., Advanced material processing with nano- and femto-second pulsed laser. *International Journal of Machine Tools and Manufacture* **48** (2008), 220–227.

[21] Crawford T.H.R., Borowiec A. and Haugen H.K., Femtosecond laser micromachining of grooves in silicon with 800 nm pulses. *Applied Physics A: Materials Science & Processing* **80** (2005), 1717–1724.

[22] Yan Y., Li L., Sezer K., Wang W., Whitehead D., Ji L., Bao Y., and Jiang Y., CO2 laser underwater machining of deep cavities in alumina. *Journal of the European Ceramic Society* **31** (2011), 2793–2807.

[23] Zheng Q., Fan Z., Jiang G., Pan, A., Yan Z., Lin Q., Cui J., Wang W. and Mei X., Mechanism and morphology control of underwater femtosecond laser micro grooving of silicon carbide ceramics. *Optics Express* **27** (2019), 26264-26280.

[24] Muhammad N. and Li L., Underwater femtosecond laser micromachining of thin nitinol tubes for medical coronary stent manufacture. *Applied Physics A: Materials Science & Processing* **107** (2012), 849–861.

[25] Mehrafsun S. and Messaoudi H., Dynamic process behavior in laser chemical micro machining of metals. *Journal of Manufacturing and Materials Processing* **2** (2018), 54.

[26] Zhang G., Duan Z., Wang Q., Li L., Yao W. and Liu C., Electrical potential induced switchable wettability of super-aligned carbon nanotube films. *Applied Surface Science* **427** (2018), 628–635.